

Agegraphic dark energy from entropy of the anti-de Sitter black hole

Qihong Huang^{1a} and He Huang²

¹ *School of Physics and Electronic Science,
Zunyi Normal University, Zunyi, Guizhou 563006, China*

² *College of Mechanical and Electrical Engineering,
Jiaxing Nanhu University, Jiaxing, Zhejiang 314001, China*

Abstract

In this paper, we analyze the agegraphic dark energy from the entropy of the anti-de Sitter black hole using the age of the universe as the IR cutoff. This model realizes the whole evolution of the universe, including the late-time accelerated expansion, and is consistent with observational Hubble data. Although it asymptotically approaches the standard Λ CDM model in the future, statefinder analysis shows that late-time deviations allow the two models to be distinguished.

^a Corresponding author: huangqihongzynu@163.com

I. INTRODUCTION

Observational data confirm that the universe has been undergoing a phase of accelerated expansion [1–6]. Why the universe is undergoing accelerated expansion in its present epoch remains one of the most enduring mysteries in cosmological research. To explain this phenomenon, dark energy has been proposed. The simplest candidate of dark energy is Λ CDM model. Although the Λ CDM model matches current cosmological observations [7] quite well, it faces the fine-tuning problem [8] and the coincidence problem [9]. Therefore, many dark energy models have been proposed to explain the current accelerated expansion, with major models including quintessence [10–12], phantom [13, 14], quintom [15–17], k-essence [18, 19], Chaplygin gas [20], agegraphic dark energy [21–23], and holographic dark energy [24–27].

A viable dark energy model must account for both the current accelerated expansion and the complete cosmic evolutionary sequence. Specifically, the universe requires an initial radiation dominated epoch, followed by a matter dominated epoch enabling large-scale structure formation, and culminating in dark energy dominance. To characterize the evolutionary behavior of a given cosmological model, dynamical analysis is applied. This method identifies critical points in the phase space where a stable fixed point, which is an attractor, represents dark energy dominated epoch, while the sequence of cosmological stages are marked by other key points [28]. When this method is applied to HDE models, it has achieved significant success [29–40].

The holographic dark energy (HDE) [25, 26, 41], which is based on the holographic principle, posits that the maximum information entropy of a region is bounded by its surface area [42, 43] and is another prominent candidate of dark energy. When the Bekenstein entropy is chosen as horizon entropy and the Hubble horizon as infrared(IR) cutoff, the primary HDE was proposed [24–26]. However, the primary HDE cannot describe the whole evolution of the universe [26, 27]. To solve this problem, different IR cutoffs and interactions between dark matter and dark energy are taken into consideration, leading to the proposal of different HDE models [27].

By choosing the age of the universe as the IR cutoff, the agegraphic dark energy (ADE)

model was proposed [23]. ADE models are established on the Károlyházy relation combined with the time-energy uncertainty, with their energy density sharing the same structure as that of the HDE model in formulation. Although the original ADE model can prevent the causality issue and lead to accelerated expansion, it cannot match the matter-dominated era in the early universe and mimic the cosmological constant behavior in later stages. Subsequently, these problems are solved by changing the cosmic time to the conformal time as the IR cutoff, and a new ADE model is proposed [22]. Then, ADE attracts a lot of attention and is widely studied in theory [45–67]. Recently, based on the entropy of an anti-de Sitter black hole with the Hubble horizon as the IR cutoff, a new HDE model was proposed [44], which not only realizes the late-time acceleration but also can describe the entire evolutionary history of the universe. Furthermore, slow-roll inflation and reheating naturally emerge within this HDE framework [68]. Motivated by the results of this new HDE, we choose the age of the universe as the IR cutoff and analyze agegraphic dark energy from the entropy of the anti-de Sitter black hole (ADEADS), and discuss whether ADEADS model can realize the late-time accelerated expansion and describe the entire evolutionary history of the universe; and if ADEADS model achieves these goals, whether it can be distinguished from the standard Λ CDM model.

The paper is organized as follows: In Section II, we present the model of ADEADS model. In Section III, we analyze the evolution of universe in ADEADS model. In Section IV, we examine the Hubble diagram in ADEADS model. In Section V, we discuss the dynamical behavior of ADEADS model. In Section VI, we adopt statefinder pairs to distinguish ADEADS model from the standard Λ CDM model. Finally, our main conclusions are presented in Section VII.

II. MODEL

Using the entropy of anti-de Sitter black hole, the holographic dark energy density is given by [44]

$$\rho_L = \frac{3}{\kappa^2} b^2 \left(\frac{1}{L^2} + \Lambda \right), \quad (1)$$

where $\kappa^2 = 8\pi G$, b is a dimensionless parameter and takes the value in the range $0 < b^2 < 1$, and Λ denotes the cosmological constant, which provides a possibility of obtaining the late-time acceleration of the universe. For $\Lambda = 0$, the energy density of ADEADS reduces to that of the original agegraphic dark energy [23], which cannot mimic the cosmological constant in late-time. Choosing the age of the universe

$$T = \int_0^a dt = \int_0^a \frac{da}{aH}, \quad (2)$$

as the IR cutoff, where a is the scale factor, t denotes cosmic time, and H represents the Hubble parameter, and the energy density of ADEADS takes the form

$$\rho_{de} = \frac{3}{\kappa^2} b^2 \left(\frac{1}{T^2} + \Lambda \right), \quad (3)$$

Considering a homogeneous and isotropic Friedmann-Robertson-Walker universe with the line element

$$ds^2 = -dt^2 + a^2(t)(dr^2 + r^2 d\Omega^2), \quad (4)$$

and the Friedmann equation is given as

$$H^2 = \frac{\kappa^2}{3} (\rho_r + \rho_m + \rho_{de}), \quad (5)$$

where ρ_r , ρ_m , and ρ_{de} denote the energy densities of pressureless matter, radiation, and ADEADS, respectively, and their conservation equations are

$$\dot{\rho}_r + 3H\rho_r = 0, \quad (6)$$

$$\dot{\rho}_m + 3H\rho_m = 0, \quad (7)$$

$$\dot{\rho}_{de} + 3H(1 + \omega_{de})\rho_{de} = 0, \quad (8)$$

with ω_{de} as the equation of state parameter and satisfying $p_{de} = \omega_{de}\rho_{de}$. To analyze the evolution of the universe, we introduce the following dimensionless variables

$$\Omega_r = \frac{\kappa^2 \rho_r}{3H^2}, \quad \Omega_m = \frac{\kappa^2 \rho_m}{3H^2}, \quad \Omega_{de} = \frac{\kappa^2 \rho_{de}}{3H^2}, \quad (9)$$

the Friedmann equation (5) can be rewritten as

$$\Omega_r + \Omega_m + \Omega_{de} = 1. \quad (10)$$

Combining Eqs. (5), (6), (7), (8), and (10), we obtain

$$\frac{\dot{H}}{H^2} = \frac{1}{2} \left[\Omega_m + (1 - 3\omega_{de})\Omega_{de} \right] - 2, \quad (11)$$

and the deceleration parameter q is given by

$$q = -1 - \frac{\dot{H}}{H^2}. \quad (12)$$

Using Eqs. (7), (8), (10), and (11) and the definition $' = \frac{d}{d(\ln a)}$, the automatic dynamical equations for this system can be written as

$$\Omega'_m = [(3\omega_{de} - 1)\Omega_{de} - \Omega_m + 1]\Omega_m, \quad (13)$$

$$\Omega'_{de} = [(3\omega_{de} - 1)(\Omega_{de} - 1) - \Omega_m]\Omega_{de}, \quad (14)$$

$$\xi' = \left[2 - \frac{1}{2}(\Omega_m + (1 - 3\omega_{de})\Omega_{de}) \right] \xi - \xi^2, \quad (15)$$

with

$$\omega_{de} = -1 + \frac{2}{3}b^2 \frac{\xi^3}{\Omega_{de}}, \quad (16)$$

and

$$\xi = \frac{1}{HT}. \quad (17)$$

III. EVOLUTION OF UNIVERSE

To analyze the evolution of the universe in ADEADS model, we adopt $\Omega_r^0 = 0.0001$, $\Omega_m^0 = 0.3111$, $\Omega_D^0 = 0.6888$, and $H_0 = 67.66 \text{ km s}^{-1} \text{ Mpc}^{-1}$ [7] as the initial conditions throughout this paper. Then, solving Eqs. (13), (14), and (15) numerically with different b^2 and α , where $\alpha = \frac{\Lambda}{H_0^2}$, we obtain the evolution curves for Ω_{de} , ξ , ω_{de} , and q , which are depicted in Figs. (1), (2), and (3). From the left panel of Fig. (1), it can be observed that Ω_{de} approaches 1 as the redshift decreases, which indicates that the universe is dominated by ADEADS during its late-time evolution. In the right panel of Fig. (1), we choose $b^2 = 0.6$, $\alpha = 0.8$ as an example and plot the evolutionary curves of Ω_r , Ω_m , and Ω_{de} , which show that the whole evolution of the universe can be described by this model. Fig. (2) shows that ξ satisfies $\xi \geq 0$, evolves at 0, departs from it, and converges to 0 again. The left panel of

Fig. (3) indicates that ADEADS behaves as quintessence, and ω_{de} starts at -1 , evolves away from it, and eventually approaches -1 again, mimicking a cosmological constant during the late-time evolution. The right panel of Fig. (3) shows that the late-time acceleration can be realized, and a suitable range for the transition redshift ($0.48 \leq z_t < 1$) is obtainable for the cases $b^2 = 0.2, 0.4, 0.6, 0.8$.

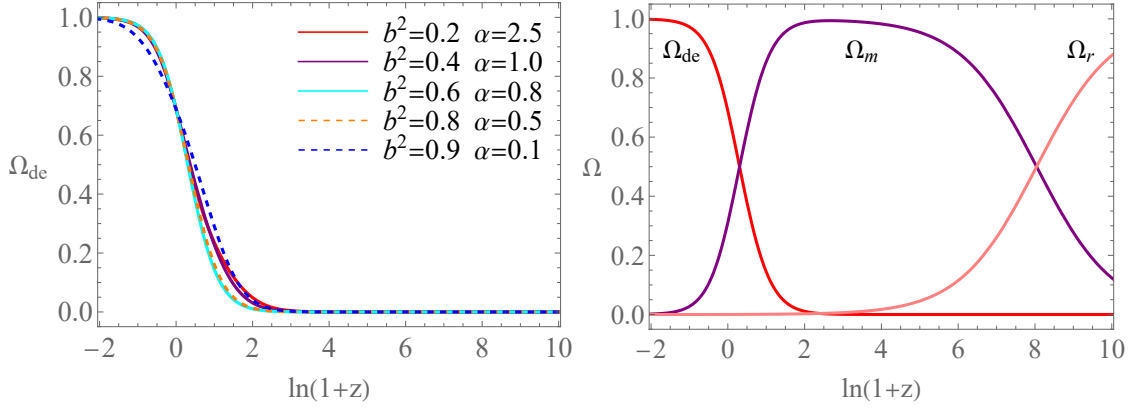


FIG. 1. Evolution curves of Ω_{de} and Ω versus redshift parameter $\ln(1+z)$. The right panel is plotted for $b^2 = 0.6, \alpha = 0.8$.

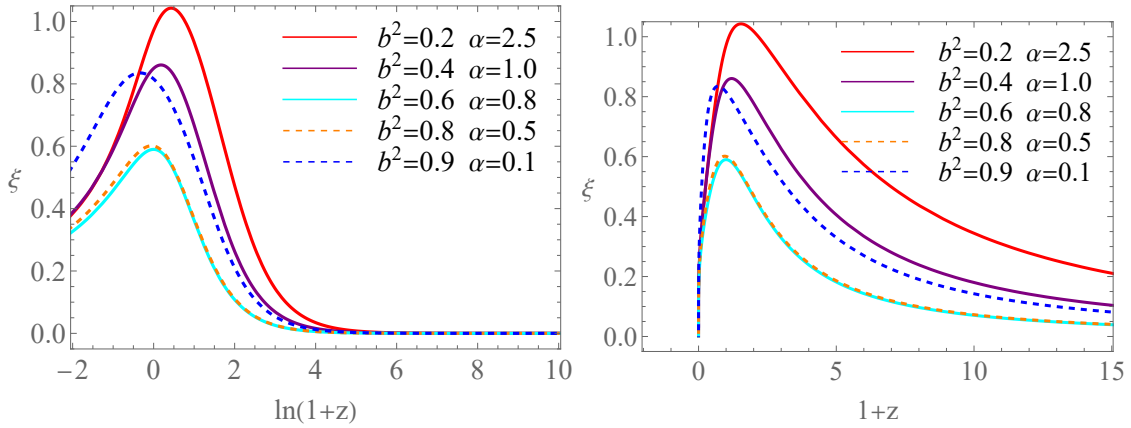


FIG. 2. Evolution curves of ξ versus redshift parameter $\ln(1+z)$ and $1+z$.

Thus, based on the above results, as both q and ω_{de} approach -1 , the current cosmic acceleration occurs naturally, with ADEADS mimicking a cosmological constant. Eventually,

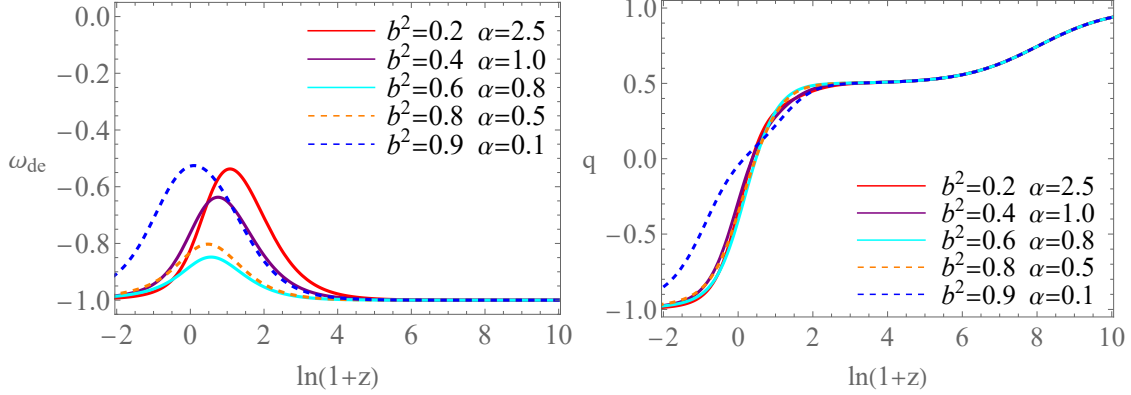


FIG. 3. Evolution curves of ω_{de} and q versus redshift parameter $\ln(1+z)$.

the universe evolves into a phase described by the standard Λ CDM model, and the whole evolution of the universe can be described by this model, as is shown in the right panel of Fig. (1).

IV. HUBBLE DIAGRAM

In the previous section, we have analyzed the evolution of the universe in ADEADS model for some cases. Whether these cases can be supported by the Hubble observational data is investigated in this section. To achieve this objective, we present the evolutionary curves of the Hubble parameter H in Fig. (4), where the error bars correspond to the observational Hubble parameter data [69, 70], and the black line denotes the standard Λ CDM model. This figure shows that although the evolutionary curves of the Hubble parameter H in ADEADS model for these special cases slightly depart from the standard Λ CDM model, they are in good agreement with observations. An increased b^2 requires a decreased α to be consistent with the observations.

In addition, a turning point in the Hubble diagram $H(z)$ is found in the holographic dark energy model with the future event horizon as the IR cutoff [71], and it can be circumvented in the Barrow holographic dark energy model [39]. For the selected cases in ADEADS model, the turning point exists at $b^2 = 0.9, \alpha = 0.1$, while it is nonexistent for the other cases.

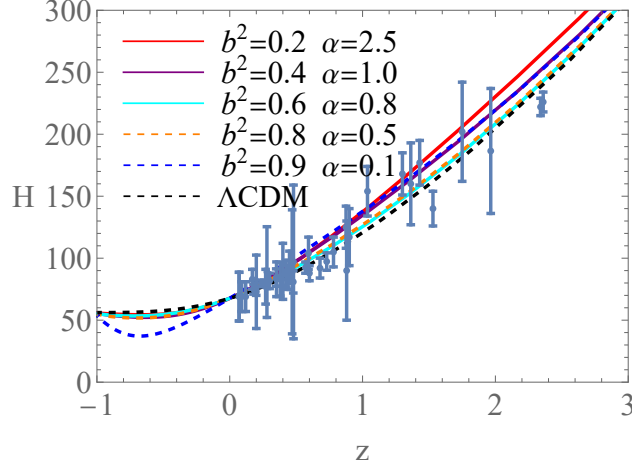


FIG. 4. Evolution curves of H .

V. DYNAMICAL ANALYSIS

In the section prior to the previous one, we have discussed the evolution of the universe in ADEADS model and found that it can describe the whole evolution of the universe and mimic a cosmological constant. In this section, we will investigate the dynamical behavior of ADEADS by adopting the dynamical system analysis [28, 36, 39, 72–82]. The critical points of the autonomous system can be obtained by solving

$$\Omega'_m = \Omega'_{de} = \xi' = 0. \quad (18)$$

For the autonomous systems (13), (14), and (15), we obtain seven critical points. Due to the physical constraint $\xi \geq 0$ in this model, one critical point with a negative ξ is discarded. The remaining six critical points are shown in Table I. Among them, points P_1, P_2, P_3 require $\xi = 0$, a condition that asymptotically holds for most of the evolutionary epoch of the universe, as shown in Fig. (2). Point P_1 represents the radiation dominated deceleration epoch; point P_2 denotes the pressureless matter dominated deceleration epoch; and point P_3 is an acceleration epoch dominated by ADEADS, with ADEADS behaving as the cosmological constant since $\omega_{de} = -1$ in these cases. Points P_4, P_5 , and P_6 are determined by the value of b^2 . For $b^2 = \frac{4}{9}$, P_4 denotes an ADEADS dominated deceleration epoch; whereas when b^2 takes small values,

TABLE I. Critical points and stability conditions of ADEADS.

<i>Label</i>	<i>Points</i> ($\Omega_m, \Omega_{de}, \xi$)	Ω_r	ω_{de}	q	<i>Eigenvalues</i>	<i>Conditions</i>	<i>Points</i>
P_1	(0, 0, 0)	1	-1	1	(4, 2, 1)	<i>Always</i>	<i>Unstable point</i>
P_2	(1, 0, 0)	0	-1	$\frac{1}{2}$	$(3, \frac{3}{2}, -1)$	<i>Always</i>	<i>Saddle point</i>
P_3	(0, 1, 0)	0	-1	-1	(-4, -3, 0)	<i>Always</i>	<i>Stable point</i>
P_4	$(1 - \frac{9}{4}b^2, \frac{9}{4}b^2, \frac{3}{2})$	0	0	$\frac{1}{2}$	$(3, -1, -\frac{3}{2} + \frac{27}{8}b^2)$	<i>Always</i>	<i>Saddle point</i>
P_5	(0, $4b^2$, 2)	$1 - 4b^2$	$\frac{1}{3}$	1	$(4, 1, -2 + 8b^2)$	$b^2 < \frac{1}{4}$	<i>Saddle point</i>
P_6	$(0, 1, \frac{1}{\sqrt{b^2}})$	0	$-1 + \frac{2}{3\sqrt{b^2}}$	$-1 + \frac{1}{\sqrt{b^2}}$	$(\frac{2}{\sqrt{b^2}}, -4 + \frac{2}{\sqrt{b^2}}, -3 + \frac{2}{\sqrt{b^2}})$	$\frac{4}{9} < b^2 < 1$	<i>Saddle point</i>

it denotes a pressureless matter dominated one, with ADEADS behaving as pressureless matter since $\omega_{de} = 0$ in both cases. For $b^2 = \frac{1}{4}$, P_5 represents an ADEADS dominated deceleration epoch; under small b^2 conditions, however, dominance shifts to radiation, with ADEADS behaving as radiation since $\omega_{de} = \frac{1}{3}$ in both cases.

By linearizing the autonomous system described by Eqs. (13), (14), and (15), we derive their corresponding first order differential equations. The stability of the critical points, as summarized in Tab. I, is governed by the coefficient matrix of these linearized equations. If all eigenvalues are negative, the point is a stable attractor; if all eigenvalues are positive, it becomes unstable; if there are both positive and negative eigenvalues, the point acts as a saddle. For point P_3 , the vanishing third eigenvalue characterizes it as a non-hyperbolic critical point. To analyze its stability, numerical methods can be employed to investigate the asymptotic behavior near this critical point [75–77]. In Fig. 5, we have depicted the time evolution of trajectories projected onto the Ω_m , Ω_{de} , and ξ -axis for critical point P_3 . From this figure, under initial perturbations, the trajectories converge toward point P_3 without divergence, thereby confirming that it is a stable attractor.

From Tab. I, it is observed that point P_1 is unstable, P_3 is stable, and the other points are saddle points. We have plotted the phase diagram with critical points and evolutionary trajectories in Fig. 6; the left panel displays the $(\Omega_m, \Omega_{de}, \xi)$ space configuration, while the right panel shows the projection onto the (Ω_m, Ω_{de}) plane. According to the stability of these critical points in Tab. I and Fig. 6, we can see that the universe will eventually evolve into the ADEADS dominated late-time acceleration epoch, which can mimic the cosmolog-

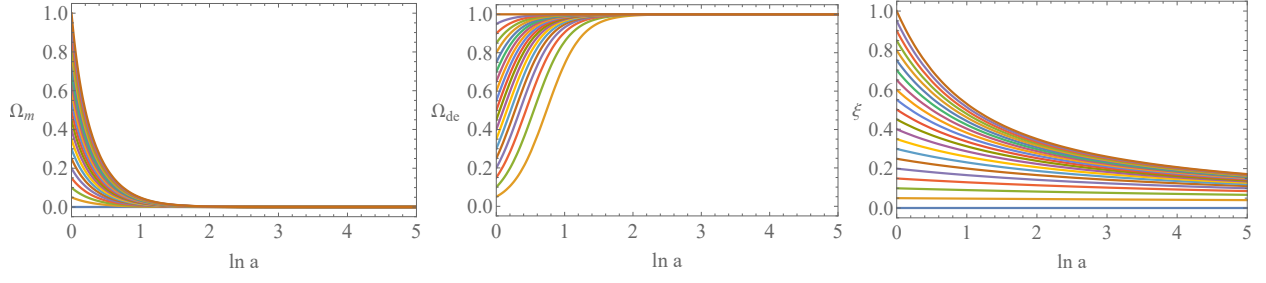


FIG. 5. Time evolution of trajectories projected on Ω_m , Ω_{de} , and ξ -axis for P_3 . These panels are plotted for $b^2 = 0.2$.

ical constant. If the universe initially evolves from the radiation dominated epoch (P_1), it can transition into the pressureless matter dominated epoch (P_2), and ultimately enter the ADEADS dominated late-time acceleration epoch (P_3); this scenario comprehensively describes the whole evolution trajectory of the universe and is graphically presented by the red curves in Fig. 6.

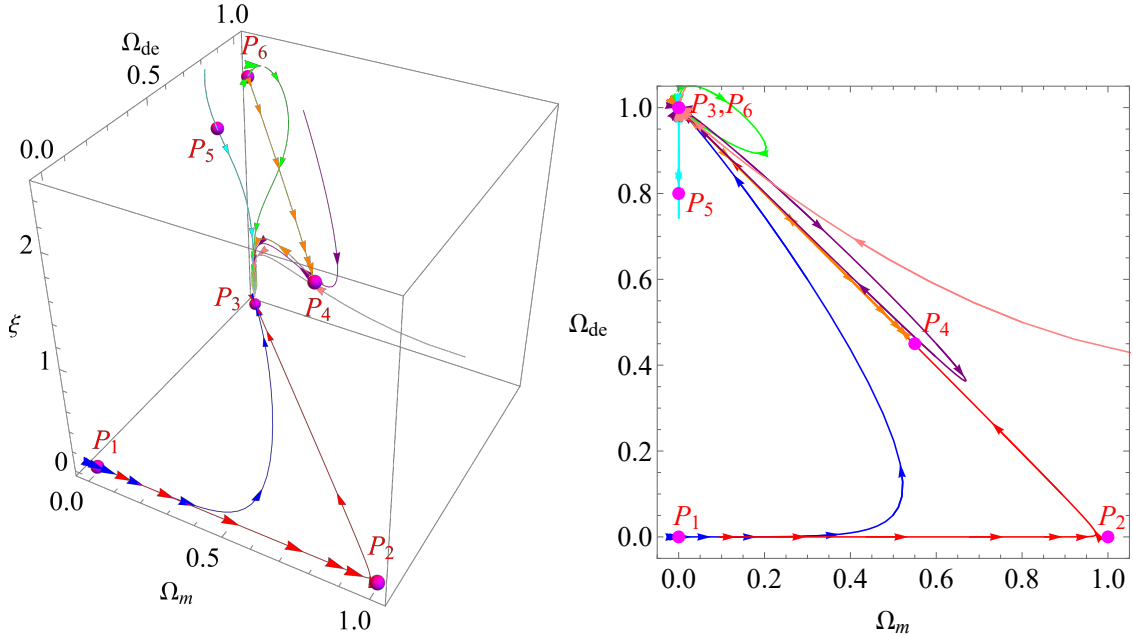


FIG. 6. Phase diagram with critical points and evolutionary trajectories. The left panel is plotted for the $(\Omega_m, \Omega_{de}, \xi)$ space, while the right one is for the (Ω_m, Ω_{de}) plane.

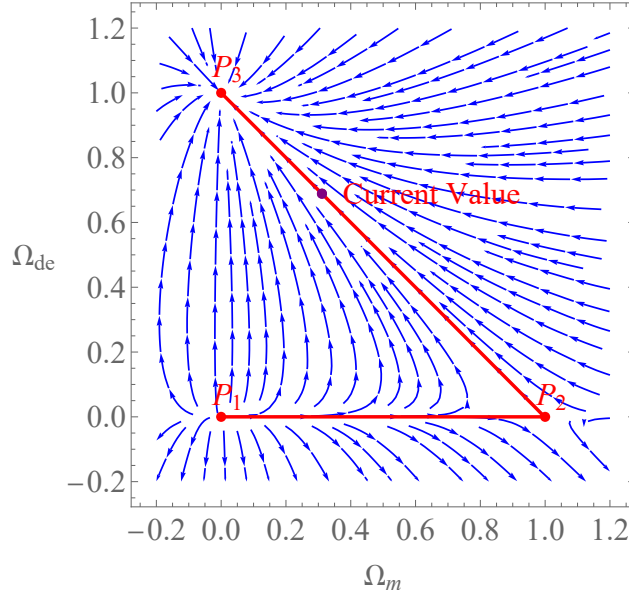


FIG. 7. Phase diagram of (Ω_m, Ω_{de}) on the $\xi = 0$ plane.

From Fig. 6, we can see that there exist three important critical points P_1, P_2, P_3 which describe the entire evolution of the universe and are located on the $\xi = 0$ plane. To intuitively investigate the dynamics of these points, the phase diagram of (Ω_m, Ω_{de}) on the $\xi = 0$ plane is shown in Fig. 7, which is plotted for $b^2 = 0.2$; the variation of b^2 will have no impact on the dynamic behavior of this system. Thus, this model is suitable for describing the entire evolutionary history of the universe, and the universe will eventually evolve into an epoch characterized by the cosmological constant Λ since ADEADS can behave as the cosmological constant at the late-time evolution.

VI. STATEFINDER ANALYSIS

According to the results in previous section, we find that ADEADS model can describe the entire evolutionary history of the universe and an attractor that behaves like the cosmological constant Λ exists in ADEADS model. To distinguish ADEADS model from the standard Λ CDM model, we employ the statefinder diagnostic pairs $\{r, s\}$ and $\{r, q\}$ developed by Sahni *et al.* [83] to analyze whether ADEADS model can be differentiated from the standard

Λ CDM model.

The statefinder parameters r and s , defined as geometric diagnostics derived exclusively from the cosmic scale factor a , are expressed as [83, 84]

$$r = \frac{\ddot{a}}{aH^3}, \quad s = \frac{r-1}{3(q-\frac{1}{2})}. \quad (19)$$

Through differentiation of Eq. (11), the statefinder parameters r and s can be expressed in terms of Ω'_m , Ω'_{de} , and ξ' . Thus, solving Eqs. (13), (14), and (15) numerically, we can obtain the evolutionary curves of the universe in the $\{r, s\}$ and $\{r, q\}$ plane.

In the left panel of Fig. (7), we plot some examples of the evolution curves for the statefinder diagnostic pair $\{r, s\}$. The green line corresponds to the Λ CDM model, with its fixed point $(0, 1)$ marked by a green dot, while other dots represent current values from respective trajectories. The evolution curves for these examples deviate from the Λ CDM model in the late-time evolution, then enter the quintessence region, and eventually evolve to the Λ CDM fixed point $(0, 1)$. In the left panel of Fig. (7), we depict another statefinder diagnostic pairs $\{r, q\}$, where the magenta dot represents the de Sitter expansion fixed point $(-1, 1)$, and the green dot denotes the standard cold dark matter fixed point $(0.5, 1)$. The evolution curves for these examples originate from the standard cold dark matter fixed point $(0.5, 1)$ and eventually converge toward the de Sitter expansion fixed point $(-1, 1)$. Thus, ADEADS model can be differentiated from the standard Λ CDM model by the statefinder diagnostic pairs $\{r, s\}$ and $\{r, q\}$.

VII. CONCLUSION

Based on the entropy of anti-de Sitter black holes with the Hubble horizon as the IR cutoff, a new HDE model has been proposed, which can realize the late-time accelerated expansion of the universe. In this paper, by choosing the age of the universe as the IR cutoff, we analyze the evolution of the universe in the ADEADS model for some examples. The results show that the ADEADS model can realize the late-time accelerated expansion and mimic the cosmological constant Λ since ω_{de} and q approach -1 , and it can describe the whole evolutionary history of the universe with radiation, pressureless matter, and ADEADS dominating

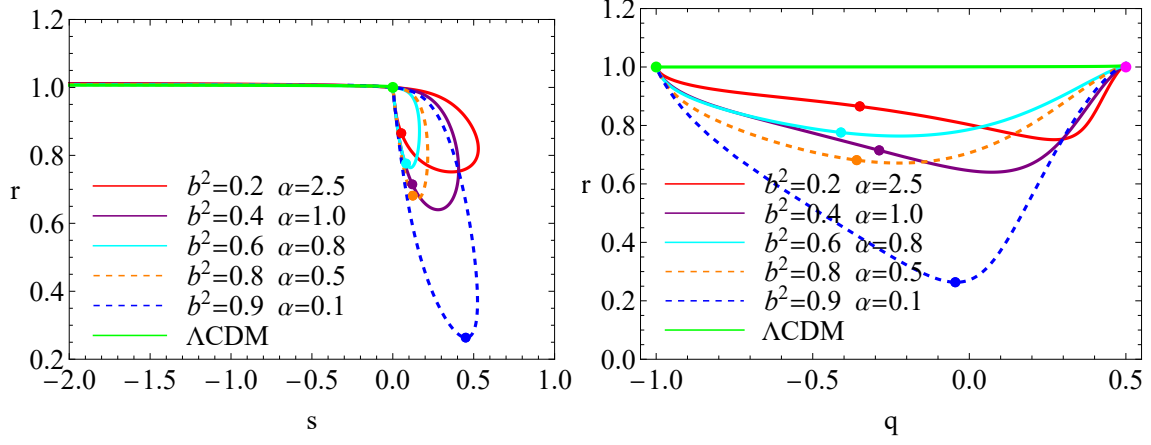


FIG. 8. Statefinder diagnostics in $\{r, s\}$ and $\{r, q\}$ plane. The dots represent the corresponding current values.

the evolution of the universe. When we check these examples using Hubble parameter data from observations, we find that the data supports them. Then, applying dynamical analysis techniques to the ADEADS model, we find that the universe will eventually evolve into an epoch characterized by the standard Λ CDM model since the attractor in the ADEADS model represents an epoch described by the cosmological constant Λ . In order to distinguish the ADEADS model from the standard Λ CDM model, we adopt the statefinder analysis method and find that the evolution curves for these examples deviate from the Λ CDM model in the late-time evolution, which indicates that the ADEADS model can be distinguished from the standard Λ CDM model. Thus, the ADEADS model, with the age of the universe as the IR cutoff, not only successfully describes the entire evolutionary history of the universe including the late-time acceleration phase but also asymptotically approaches the standard Λ CDM model, while remaining distinguishable from it through observable differences in the late universe.

ACKNOWLEDGMENTS

This work was supported by the National Natural Science Foundation of China under Grants Nos.12405081, 12265019, 11865018.

- [1] S. Perlmutter, G. Aldering, G. Goldhaber et al., *Astrophys. J.* **517**, 565 (1999).
- [2] A. Riess, A. Filippenko, P. Challis et al., *Astron. J.* **116**, 1009 (1998).
- [3] D. Spergel et al., *Astrophys. J. Suppl.* **148**, 175 (2003).
- [4] D. Spergel et al., *Astrophys. J. Suppl.* **170**, 337 (2007).
- [5] M. Tegmark et al., *Phys. Rev. D* **69**, 103501 (2004).
- [6] D. Eisenstein et al., *Astron. J.* **633**, 560 (2005).
- [7] Planck Collaboration, *A&A.* **641**, A6 (2020).
- [8] S. Weinberg, *Rev. Mod. Phys.* **61**, 1 (1989).
- [9] P. Steinhardt, L. Wang, and I. Zlatev, *Phys. Rev. D* **59**, 123504 (1999).
- [10] C. Wetterich, *Nucl. Phys. B* **302**, 668 (1988).
- [11] B. Ratra and P. Peebles, *Phys. Rev. D* **37**, 3406 (1988).
- [12] R. Caldwell, R. Dave, and P. Steinhardt, *Phys. Rev. Lett.* **80**, 1582 (1998).
- [13] R. Caldwell, *Phys. Lett. B* **545**, 23 (2002).
- [14] R. Caldwell, M. Kamionkowski, and N. Weinberg, *Phys. Rev. Lett.* **91**, 071301 (2003).
- [15] B. Feng, X. Wang, and X. Zhang, *Phys. Lett. B* **607**, 35 (2005).
- [16] B. Feng, M. Li, Y. Piao, and X. Zhang, *Phys. Lett. B* **634**, 101 (2006).
- [17] Z. Guo, Y. Piao, X. Zhang, and Y. Zhang, *Phys. Lett. B* **608**, 177 (2005).
- [18] T. Chiba, T. Okabe, and M. Yamaguchi, *Phys. Rev. D* **62**, 023511 (2000).
- [19] C. Armendariz-Picon, V. F. Mukhanov, and P. J. Steinhardt, *Phys. Rev. D* **63**, 103510 (2001).
- [20] A. Kamenshchik, U. Moschella, and V. Pasquier, *Phys. Lett. B* **511**, 265 (2001).
- [21] H. Wei and R. Cai, *Phys. Lett. B* **655**, 1 (2007).
- [22] H. Wei and R. Cai, *Phys. Lett. B* **660**, 113 (2008).

- [23] R. Cai, Phys. Lett. B **657**, 228 (2007).
- [24] A. Cohen, D. Kaplan, and A. Nelson, Phys. Rev. Lett. **82**, 4971 (1999).
- [25] S. Hsu, Phys. Lett. B **594**, 13 (2004).
- [26] M. Li, Phys. Lett. B **603**, 1 (2004).
- [27] S. Wang, Y. Wang, and M. Li, Phys. Rep. **696**, 1 (2017).
- [28] S. Bahamonde, C. Bohmer, S. Carloni, E. Copeland, W. Fang, and N. Tamanini, Phys. Rep. **775-777**, 1 (2018).
- [29] M. Setare and E. Vagenas, Int. J. Mod. Phys. D **18**, 147 (2009).
- [30] J. Liu, Y. Gong, and X. Chen, Phys. Rev. D **81**, 083536 (2010).
- [31] N. Banerjee and N. Roy, Gen. Relativ. Gravit. **47**, 92 (2015).
- [32] N. Mahata and S. Chakraborty, Mod. Phys. Lett. A **30**, 1550134 (2015).
- [33] S. Mishra and S. Chakraborty, Mod. Phys. Lett. A **34**, 1950147 (2019).
- [34] A. Bargach, F. Bargach, and T. Ouali, Nucl. Phys. B **940**, 10 (2019).
- [35] A. Tita, B. Gumjudpai, and P. Srisawad, Phys. Dark Univ. **45**, 101542 (2024).
- [36] Q. Huang, H. Huang, J. Chen, L. Zhang, and F. Tu, Class. Quantum Grav. **36**, 175001 (2019).
- [37] E. Ebrahimi, Astrophys. Space. Sci. **365**, 92 (2020).
- [38] A. Astashenok and A. Tepliakov, Int. J. Mod. Phys. D **32**, 2350058 (2023).
- [39] Q. Huang, H. Huang, B. Xu, F. Tu, and J. Chen, Eur. Phys. J. C **81**, 686 (2021).
- [40] S. Srivastava and U. Sharma, Int. J. Geom. Methods Mod. Phys. **18**, 2150014 (2021).
- [41] R. Horvat, Phys. Rev. D **70**, 087301 (2004).
- [42] E. Witten, Adv. Theor. Math. Phys. **2**, 253 (1998).
- [43] R. Bousso, Rev. Modern Phys. **74**, 825 (2002).
- [44] R. Nakarachinda, C. Pongkitivanichkul, D. Samart, L. Tannukij, and P. Wongjun, Phys. Rev. D **105**, 123524 (2022).
- [45] H. Huang, Q. Huang, and R. Zhang, Gen. Relativ. Gravit. **53**, 63 (2021).
- [46] Pankaj, B. Pandey, P. Kumar, and U. Sharma, Int. J. Mode. Phys. **31**, 2250102 (2022).
- [47] Z. Mangoudehi, Astrophys. Space Sci. **367**, 31 (2022).
- [48] U. Sharma and S. Srivastava, Mod. Phys. Lett. A **35**, 2050318 (2020).

- [49] H. Huang, Q. Huang, and R. Zhang, *Universe* **8**, 467 (2022).
- [50] A. Sheykhi and S. Ghaffari, *Phys. Dark Universe* **41**, 101241 (2023).
- [51] U. Sharma, G. Varshney, and V. Dubey, *Int. J. Mode. Phys.* **30**, 2150021 (2021).
- [52] A. Ravanpak and G. Fadakar, *Mod. Phys. Lett. A* **34**, 1950105 (2019).
- [53] M. Zadeh, A. Sheykhi, and H. Moradpour, *Mod. Phys. Lett. A* **34**, 1950086 (2019).
- [54] P. Kumar and C. Singh, *Astrophys. Space Sci.* **362**, 52 (2017).
- [55] P. Saha and U. Debnath, *Eur. Phys. J. C* **76**, 491 (2016).
- [56] J. Zhang, L. Zhao, and X. Zhang, *Sci. China Phys. Mech. Astron.* **57**, 387 (2014).
- [57] J. Zhang, Y. Li, and X. Zhang, *Eur. Phys. J. C* **73**, 2280 (2013).
- [58] H. Farajollahi, A. Ravanpak, and G. Fadakar, *Phy. Let. B* **711**, 225 (2012).
- [59] Y. Li, J. Zhang, and X. Zhang, *Chinese Phys. B* **22**, 039501 (2013).
- [60] K. Saaide, H. Sheikahmadi, and A. Mohammadi, *Astrophys. Space Sci.* **338**, 355 (2012).
- [61] H. Farajollahi, J. Sadeghi, M. Pourali, and A. Salehi, *Astrophys. Space Sci.* **339**, 79-85 (2012).
- [62] C. Sun and R. Yue, *Phys. Rev. D* **83**, 107302 (2011).
- [63] Y. Li, J. Ma, J. Cui, Z. Wang, and X. Zhang, *Sci. China Phys. Mech. Astron.* **54**, 1367 (2011).
- [64] O. Lemets, D. Yerokhin, and L. Zazunov, *JCAP* **01**, 007 (2011).
- [65] C. Sun, and Y. Song, *Mod. Phys. Lett. A* **26**, 3055 (2011).
- [66] H. Wei and R. Cai, *Phys. Lett. B* **663**, 1 (2008).
- [67] H. Wei and R. Cai, *Eur. Phys. J. C* **59**, 99 (2009).
- [68] Q. Huang, H. Huang, B. Xu, and K. Zhang, *Eur. Phys. J. C*, **85**, 395 (2025).
- [69] I. Akhlaghi, M. Malekjani, S. Basilakos, and H. Haghi, *MNRAS* **477**, 3659 (2018).
- [70] S. Cao, T. Zhang, X. Wang, and T. Zhang, *Universe* **7**, 57 (2021).
- [71] E. Colgain and M. Sheikh-Jabbari, *Class. Quantum Grav.* **38**, 177001 (2021).
- [72] P. Wu and H. Yu, *Phys. Lett. B* **692**, 176 (2010).
- [73] P. Wu and S. Zhang, *JCAP* **06**, 007 (2008).
- [74] P. Wu and H. Yu, *Class. Quant. Grav.* **24**, 4661 (2007).
- [75] J. Dutta, W. Khyllep and N. Tamanini, *Phys. Rev. D* **93**, 063004 (2016).
- [76] J. Dutta, W. Khyllep, and N. Tamanini, *Phys. Rev. D* **95**, 023515 (2017).

- [77] J. Dutta, W. Khyllep, and H. Zonunmawia, *Eur. Phys. J. C* **79**, 369 (2019).
- [78] Q. Huang, H. Huang, B. Xu, and K. Zhang, *Universe* **11**, 147 (2025).
- [79] Q. Huang, R. Zhang, J. Chen, H. Huang, and F. Tu, *Mod. Phys. Lett. A* **36**, 2150052 (2021).
- [80] Y. Huang, Q. Gao, and Y. Gong, *Eur. Phys. J. C* **75**, 143 (2015).
- [81] X. Chen, Y. Gong, and E. Saridakis, *JCAP* **04**, 001 (2009).
- [82] A. Chatterjee and Y. Gong, *Ann. Phys.* **478**, 170036 (2025).
- [83] V. Sahni, T. D. Saini, A. A. Starobinsky, and U. Alam, *JETP Lett.* **77**, 201 (2003).
- [84] P. Wu and H. Yu, *Int. J. Mod. Phys. D* **14**, 1873 (2005).